

# Perfusion in Hamster Skin Treated With Glycerol

Raiyan T. Zaman, MSE,<sup>1\*</sup> Ashwin B. Parthasarathy, MSE,<sup>1</sup> Gracie Vargas, PhD,<sup>2</sup> Bo Chen, PhD,<sup>1,3</sup> Andrew K. Dunn, PhD,<sup>1</sup> Henry G. Rylander III, MD,<sup>1</sup> and Ashley J. Welch, PhD<sup>1</sup>

<sup>1</sup>Department of Biomedical Engineering, University of Texas, Austin, Texas 78712

<sup>2</sup>Department of Neuroscience and Cell Biology and the Center for Biomedical Engineering, University of Texas Medical Branch, Galveston, Texas 77550

<sup>3</sup>Cynosure Inc., Westford, Massachusetts

**Background and Objective:** The objective of this article is to quantify the effect of hyper-osmotic agent (glycerol) on blood velocity in hamster skin blood vessels measured with a dynamic imaging technique, laser speckle contrast imaging (LSCI).

**Study Design/Materials and Methods:** In this study a dorsal skin-flap window was implanted on the hamster skin. The hyper-osmotic drug, that is, glycerol was delivered to the skin through the open dermal end of the window model. A two-dimensional map of blood flow of skin blood vessels was obtained from the speckle contrast (SC) images.

**Results:** Preliminary studies demonstrated that hyper-osmotic agents such as glycerol not only make tissue temporarily transparent, but also reduce blood flow. The blood perfusion was measured every 3 minutes for 36–66 minutes after diffusion of anhydrous glycerol. Blood flow in small capillaries was found to be reduced significantly within 3–9 minutes. Blood flow in larger blood vessels (i.e., all arteries and veins) decreased over time and some veins had significantly reduced blood flow within 36 minutes. At 24 hours, there was a further reduction in capillary blood perfusion whereas larger blood vessels regained flow compared to an hour after initial application of glycerol.

**Conclusion:** Blood flow velocity and vessel diameter of the micro-vasculatures of hamster skin were reduced by the application of 100% anhydrous glycerol. At 24 hours, capillary perfusion remained depressed. *Lasers Surg. Med.* 41:492–503, 2009. © 2009 Wiley-Liss, Inc.

**Key words:** hyper-osmotic agents; window model; speckle measurement; blood flow velocity; speckle contrast (SC); laser speckle contrast imaging (LSCI)

## INTRODUCTION

The diffusion of hyper-osmotic agents such as glycerol in skin reduces light scattering which increases the penetration depth of light. The increase in penetration depth is due to a reduction of refractive index mismatch among the cellular contents, structural components (such as collagen and elastin fibers), and extra-cellular fluid [1]. In addition, a hyper-osmotic agent such as glycerol increases the local concentration of scattering particles as a result of tissue dehydration [2]. The increase in penetration depth should enhance diagnostic (optical coherence tomography) and therapeutic (coagulation of blood vessels) procedures [3].

One side effect for some hyper-osmotic agents and particularly glycerol is the reduction in blood vessel diameter and flow velocity [1,4–7]. It is this dynamic change in tissue perfusion that is the subject of this article.

In a previous study, Vargas et al. [3] measured flow velocity of in vivo hamster skin blood vessels using Doppler Optical Coherence Tomography (DOCT) before and after 100% anhydrous glycerol application. Veins with inner diameters of 500  $\mu\text{m}$  or less were completely closed with no blood flow at 50 minutes after treating the subdermal skin with glycerol. Although blood flow through arteries decreased, some flow remained through the treatment with glycerol. The Doppler image also identified that glycerol induced a decrease in optical thickness of the connective tissue overlaying the blood vessels on the subdermal side and conformed to the shape of the blood vessels. Although, the DOCT study provided absolute blood flow velocity and morphological changes induced by glycerol for up to 50 minutes, the velocity and associated morphology were measured for only a single pair of blood vessels such as an artery and a vein. Choi et al. [8] demonstrated the application of laser speckle imaging (LSI) to an in vivo rodent dorsal skinfold model and showed LSI's potential as a wide-field microvasculature imaging modality. In this hemodynamic study, blood flow velocity was measured for up to 16 minutes after glycerol application and showed an heterogeneous decrease in blood flow with an initial decrease in venular flow and a delayed decrease in arteriolar flow of the microvasculature network of the rodent dorsal skin-fold chamber. A study by Zhu et al. [9] showed the changes in morphology of vessels and blood flow velocity of chick chorioallantoic membrane after application of hyper-osmotic agents such as glycerol and glucose. In their study, measurements were made up to 31.5 minutes and one additional measurement at 48 hours after the

Contract grant sponsor: National Science Foundation; Contract grant number: UTA06-688; Contract grant sponsor: Caster Foundation.

\*Correspondence to: Raiyan T. Zaman, MSE, Department of Biomedical Engineering, The University of Texas at Austin, 1 University Station C0800, BME 1.344, Austin, TX 78712-0238. E-mail: raiyan\_zaman@yahoo.com

Accepted 2 July 2009

Published online 15 August 2009 in Wiley InterScience (www.interscience.wiley.com).

DOI 10.1002/lsm.20803

application of hyper-osmotic agents such as glycerol and glucose. Both agents reduced local blood flow velocity and at 48 hours there was some recovery. However, the hemodynamics of hamster skin blood vessels and their morphological changes as a function of vessel type and size after application of a hyper-osmotic agent such as glycerol from 0 to 66 minutes and at 24 hours has not been investigated in the hamster model using laser speckle contrast imaging (LSCI) technique. Our research extends LSCI measurements of dynamics in morphology and blood flow velocity of the hamster skin microvasculature such as arteries, veins, and capillaries over short term (0–66 minutes) and long term (24 hours) after application of glycerol and both natural and saline induced recovery.

To investigate the transport of hyper-osmotic agents across skin and microcirculation on a full thickness of skin from both the epidermal and sub-dermal side of skin, a series of in vivo experiments were performed using a hamster dorsal skin-flap window model. LSCI provided a two-dimensional (2D) map of blood flow in skin blood vessels during and after the diffusion of glycerol in the skin. The blood flow map was obtained using a dynamic imaging technique—LSCI [10,11].

### SPECKLE CONTRAST (SC) IMAGING

Laser speckle is a random interference pattern caused by coherent addition of scattered laser light. Motion of the scattering particles causes blurring or de-correlation of the speckle pattern. Quantification of the extent of blurring provides a measure of speed of the moving scatterers. This measurement is done by calculating speckle contrast (SC). The local SC is defined as the ratio of the standard deviation,  $\sigma_s$ , to the mean intensity of the back scattered light from the surface of the sample,  $\langle I \rangle$ , in a small region of the image [10],

$$SC = \frac{\sigma_s}{\langle I \rangle} \quad (1)$$

To ensure accurate determination of  $\sigma_s$  and  $\langle I \rangle$ , the size of the region over which the SC is computed must be large enough to contain a sufficient number of pixels: however, not so large that significant spatial resolution is lost. SC values range between 0 and 1 and are inversely related to blood flow [12]. An SC of 1 indicates that there is no blurring of the speckle pattern and, therefore, no motion, whereas, an SC of 0 means that the scatterers are moving fast enough to average out all of the speckles. However, in practice it is never possible to get absolute 0 and speckle averaging effects prevent obtaining an SC of 1 for a completely static sample.

To quantify blood flow the SC values can be converted to intensity correlation decay times,  $\tau_c$ , using

$$SC = \frac{\sigma_s}{\langle I \rangle} = \left[ \frac{\tau_c}{2T} \left\{ 1 - \exp\left(\frac{-2T}{\tau_c}\right) \right\} \right]^{1/2} \quad (2)$$

Yuan et al. [13] suggest that an integration time ( $T$ ) of 5 milliseconds is appropriate for physiological flow measurements.

## MATERIALS AND METHODS

### Animal Preparation

Male Golden Syrian hamsters ( $n = 13$ ) weighing 120–150 g obtained from Harlan Sprague–Dawley, were used for the experiments. Six out of thirteen hamsters were used in the control group study. All experimental procedures were conducted according to protocols approved by the Animal Care Committee of the University of Texas at Austin. Hamsters were anesthetized with IP 200 mg/kg Ketaset and 10 mg/kg Xylazine. The depth of the anesthesia was monitored throughout the procedure by checking heart rate, breathing, and toe pinch and by supplements of one half of the initial dose of Ketaset every 1 hour. Body temperature was kept constant at 37°C with a heating pad designed for small animal experiments. All hamsters were held on the heating pad with two pieces of surgical tape (one at the thoracic area and other at the pelvic area) to minimize any movement. In addition, two velcro straps held the heating pad at a fixed position on a lab jack and the lab jack on an optical table. These constraints fixed the animal position each time a LSCI measurement was performed.

### Surgical Procedure

To investigate the transport of a hyper-osmotic agent across skin and microcirculation on a full thickness of skin from both the epidermal and subdermal side of skin, a series of in vivo experiments were performed using a hamster dorsal skin-flap window model. Papenfuss et al. [14] first developed the model for the simultaneous observation of the sub-dermal and epidermal sides of skin. This allowed a direct in vivo view of dermal blood vessels while having access to the epidermal side of the skin. Prior to surgery the dorsal area of a hamster was shaved and epilated. The dorsal skin was raised from the mid-section of the body and sutured to a C-clamp to hold the skin away from the body. A circular section was cut from one section of skin, leaving the facing section exposed on its sub-dermal side. An aluminum chamber was sutured to both sides of the skin. The final preparation viewed from the epidermal (left) and sub-dermal side (right) is shown in Figure 1. Before LSCI measurements, the window (on the sub-dermal side) was filled with either phosphate buffer saline

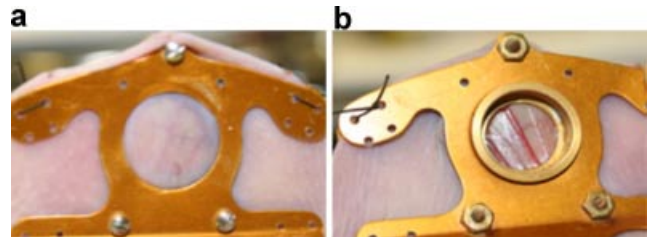


Fig. 1. Hamster dorsal skin flap window preparation showing a single thickness of hamster skin. **a**: Shown from the epidermal side. **b**: Shown from the exposed sub-dermal side. In this particular window preparation direct visualization of blood vessels is allowed.

(PBS) for control experiments or 100% anhydrous glycerol for the experimental group. The total volume of fluid was approximately 0.7 ml and 0.2 ml was replenished every 10 minutes until 36, 60, or 66 minutes. All experiments began 5–10 minutes after the completion of surgery.

### Experimental Procedure

**Control group study.** In the control group study, hamsters ( $n = 6$ ) were divided into two groups based on different end points. After applying PBS solution, hamsters from C1 ( $n = 3$ ) were observed for up to 60 minutes and group C2 ( $n = 3$ ) was observed for 60 minutes and then at 24 hours. The PBS solution was not removed from the window before the glass was placed after the initial measurements (60 minutes) and no additional solution was added for the 24 hour experiment. All hamsters from the experimental and control groups were euthanized according to an approved protocol.

**Experimental group study.** Blood flow velocity was measured every 3 minutes for 36, 60, or 66 minutes using the LSCI technique. An additional 24 hours measurement was made on some of the animals. Three measurements were taken to allow a statistical analysis on the 24 hours group. For both experimental and control group studies, we started the experiment with the lowest observation time and then increased gradually. Thus, the hamsters ( $n = 7$ ) in the experimental group were divided into three groups—E1, E2, and E3 based on three different end points. LSCI measurements every 3 minutes were made for 36 minutes in group E1 ( $n = 2$ ), for 66 minutes in group E2 ( $n = 2$ ), and

for 60 minutes in Group E3 ( $n = 3$ ). An additional 24 hours measurement was made for Group E3. For E3, after the initial measurements (60 minutes), a round thin glass was placed into the window over the cutout section of the skin to prevent the tissue from dehydrating. While animals were kept overnight at Animal Resource Center at the University of Texas the anhydrous glycerol was not removed from the window before the glass was placed. The thin glass was removed but no glycerol was added for the 24 hours LSCI measurement. A new bottle of glycerol was opened after each experimental group to prevent absorption of water from the atmosphere. All experiments for a given group were completed within a week after opening a bottle of glycerol.

**Speckle imaging system.** The instrument (see Fig. 2) for the LSCI measurements used in this experiment was developed by Dunn et al. [15] A diode laser beam (Sharp DL7140;  $\lambda = 780$  nm, 30 mW; Thorlabs, Newton, NJ) was collimated (collimating lens C240-TM; Thorlabs) and directed toward the sample. The lens was positioned approximately 10 cm above the area of interest and the lens was adjusted to provide even illumination of 1 cm diameter window on the sub-dermal side of the hamster skin. The illuminated area was imaged onto a CCD camera (Basler 602F, Basler Vision Technologies, Ahrensburg, Germany) through a zoom lens. Conversion of raw speckle images into a 2D pseudo blood flow SC map (see Figs. 3c–d and 4a–h) was constructed by custom written software based on Equation (1). Equation (2) was used to obtain  $\tau_c$  of flow. Five milliseconds interval was used for the

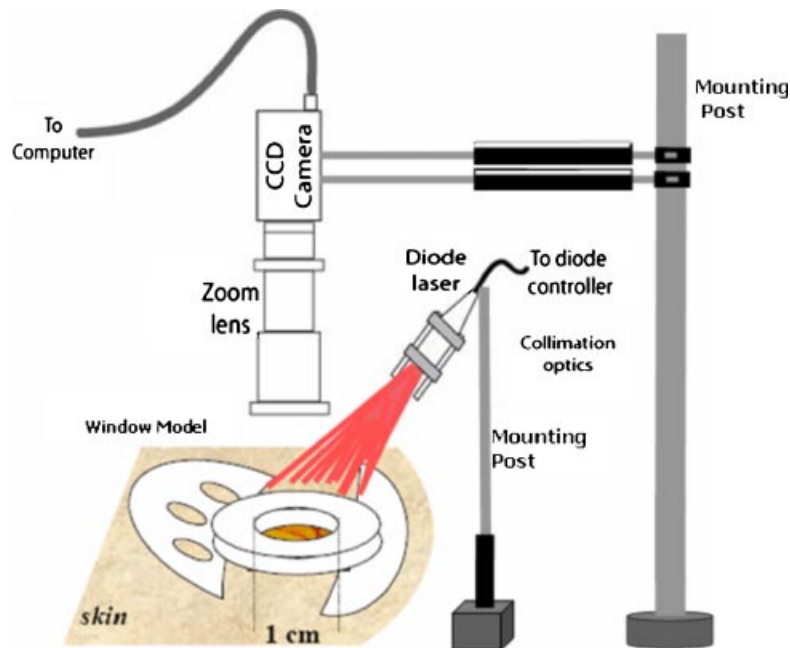


Fig. 2. Schematic illustration of the instrumentation setup for speckle imaging of skin blood flow. A laser diode beam is expanded to illuminate a 1 cm diameter window on the sub-dermal skin, which is imaged onto the CCD camera. The computer acquires raw speckle images and computes relative skin blood flow maps. [Figure can be viewed in color online via [www.interscience.wiley.com](http://www.interscience.wiley.com).]

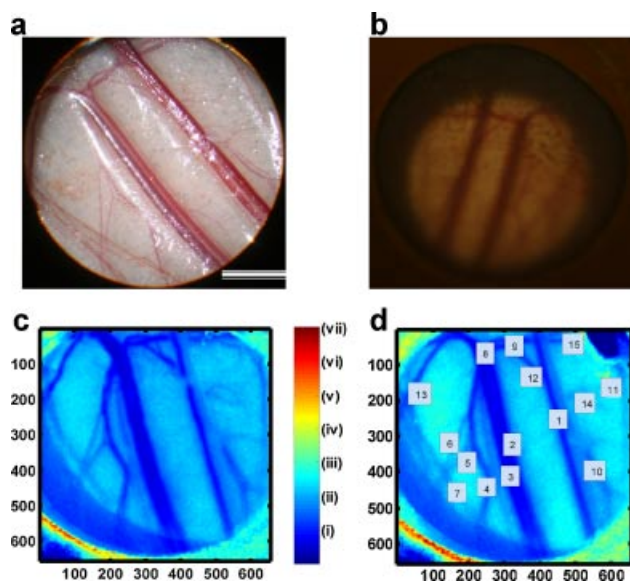


Fig. 3. Photographs of a dorsal skin flap window preparation from one of the hamster from the experimental Group I (E1) (scale bar: 0.25 cm) showing the (a) sub-dermal, (b) epidermal side of the window, (c) SC images represent (i) fastest blood velocity or lowest SC, (ii) slower blood velocity, (iii) no blood flow, (iv)–(vii) outside the window model, (d) numbered microvasculature for identification and analysis. The darker area of the SC image represents blood vessels by black = 0 and white = 1 for speckle contrast. [Figure can be viewed in color online via [www.interscience.wiley.com](http://www.interscience.wiley.com).]

exposure duration of the camera. The blood flow velocity in microvasculature was assumed to be inversely proportional to  $\tau_c$ . The velocity of the blood vessels was normalized with the velocity at 0 minute (immediately after the application of glycerol or PBS).

**Photography of hamster dorsal skin treated with glycerol or PBS solution.** With the window in the horizontal plane, an EOS digital SLR camera (Digital Rebel XT Canon Japan) attached to a surgical microscope (Topcon OMS75) was used to photograph the skin in the dorsal skin flap window preparation from the sub-dermal side. The epidermal side was imaged with a special lens (FUJINON-TV 1:1.8/75, Fuji Photo Optical Co., Saitama City, Saitama, Japan) connected with an Olympus CAMADIA C-3040ZOOM digital camera (Olympus Optical Co., LTD, Tokyo, Japan). The camera shutter was triggered using software (DSLR Remote Pro version 1.3.2, Breeze Systems). To enhance images a single layer of damp white gauze was placed on the sub-dermal side for epidermal photographs and vice versa. Photographs from the epidermal and sub-dermal sides of the native in vivo and treated skin with glycerol or saline solution were captured every 3 minutes (at the same time of LSCI measurements). Photographs (see Fig. 3a) provide a measure of vessel diameter and along with sub-dermal visualization of the skin allowed identification if a vessel was an artery, vein, or capillary.

**Diameter measurement of blood vessels.** Blood vessel's outer diameter was measured from the sub-dermal photograph using custom written software. The vessel diameter was measured at each position where the blood

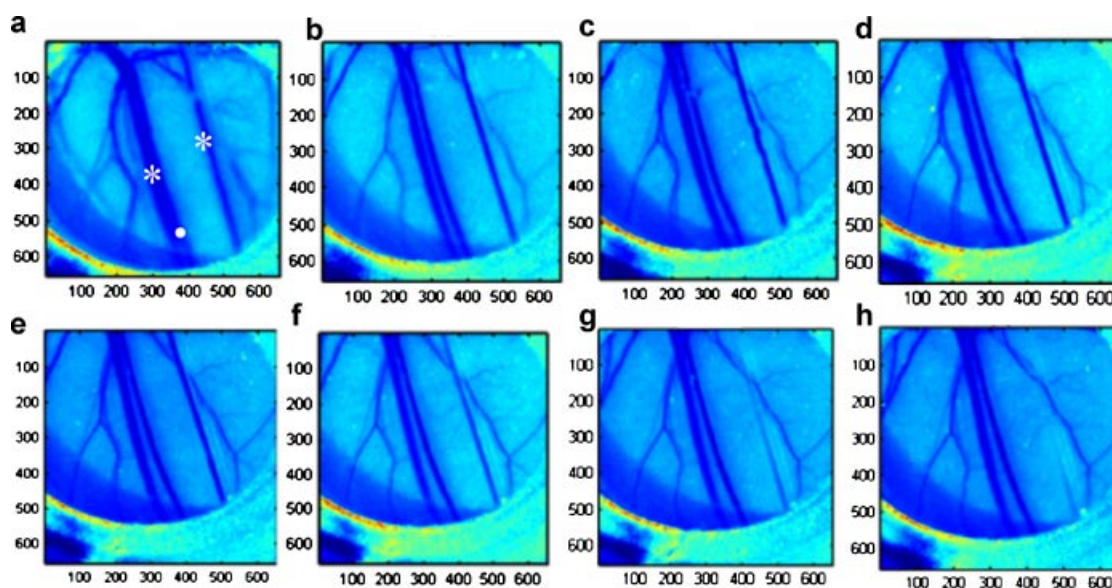


Fig. 4. SC images of the sub-dermal blood vessels of one of the hamsters from the experimental Group 1 (E1) after application of anhydrous glycerol: (a) 0 minute, (b) 3 minutes, (c) 9 minutes, (d) 15 minutes, (e) 24 minutes, (f) 27 minutes, (g) 30 minutes, and (h) 36 minutes. Positions 1 and 3 of Figure 3d are veins highlighted with asterisk and position 2 of Figure 3d is an artery highlighted with a solid circle. Same color bar from Figure 3 applies to this figure. The darker area of the SC image represents blood vessels by black = 0 and white = 1 for speckle contrast. [Figure can be viewed in color online via [www.interscience.wiley.com](http://www.interscience.wiley.com).]

flow velocity was measured using the LSCI technique. The diameter was measured in small segments where the blood vessels are in a straight line. An edge detection Randon function was implemented in a form of Hough [16] transformation to detect the diameter of these small straight segments of the microvasculature. The motivation for using the Hough transformation was to detect the edge of the blood vessels which could be in arbitrary shape. The average diameter of the arteries and veins of all seven hamsters was calculated by taking the average diameter of these small segments. The arteries and veins were identified as small or large based on their vessel diameter. Thus, individual standard deviation was calculated for these arteries and veins.

**Blood flow velocity measurement of blood vessels.** Blood flow velocity was measured from approximately two arteries, two veins, and four capillaries from each hamster model. However, these numbers varied slightly due to the individual hamster's physical modality. Only one position was selected for each microvasculature to measure the blood flow using LSCI technique. To calculate the blood flow velocity within the microvasculature (see Fig. 5), a  $5 \times 5$  square pixel subset from the entire pixels was chosen that fit entirely inside larger vessels (arteries and veins) from the 2D map of the SC values that correspond to  $76 \times 76 \mu\text{m}^2$  area. The area of  $76 \times 76 \mu\text{m}^2$  was

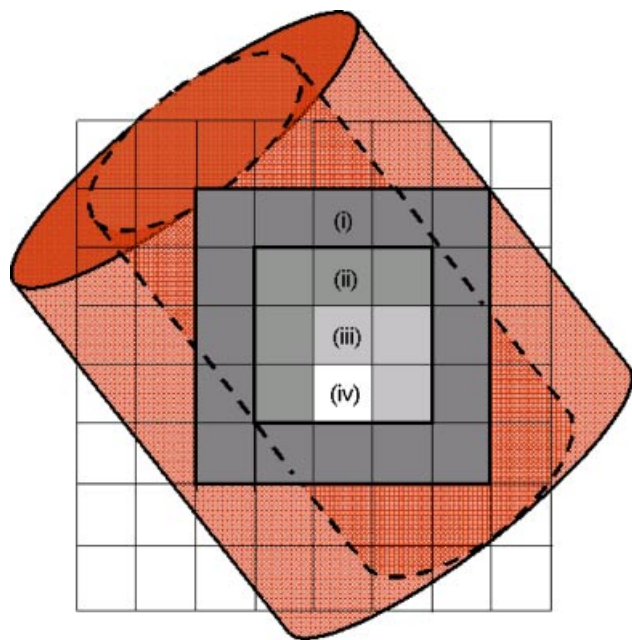


Fig. 5. A subset of  $8 \times 8$  pixels are shown from a  $656 \times 656$  area of pixels of an SC image. Selection of subset of pixel size (i)  $5 \times 5$  represents  $76 \times 76 \mu\text{m}^2$  area inside larger blood vessels such as arteries and veins, (ii)  $3 \times 3$  represents  $45.6 \times 45.6 \mu\text{m}^2$  area inside larger blood vessels with diameter  $< 76 \mu\text{m}$ , (iii)  $2 \times 2$  represents  $30.4 \times 30.4 \mu\text{m}^2$  area inside capillaries, and (iv)  $1 \times 1$  represents  $15.2 \times 15.2 \mu\text{m}^2$  area inside capillaries to calculate blood flow velocity measurements as a function of vessel size. [Figure can be viewed in color online via [www.interscience.wiley.com](http://www.interscience.wiley.com).]

chosen to measure the blood velocity at the central part of arteries and veins as most of the larger microvasculature were much larger than this chosen area. However, when the diameter of the blood vessels decreased and become smaller than this selected area due to vasoconstriction from glycerol application, a  $45.6 \times 45.6 \mu\text{m}^2$  area ( $3 \times 3$  square area) within the selected  $5 \times 5$  square area of pixels was chosen in the 2D map. Thus, only 35% of the original selected area of the 2D map corresponded to the velocity-induced SC changes when the larger blood vessel diameter decreased due to glycerol application. This measuring technique was adopted to avoid capturing any SC values from the surrounding areas which did not represent flow within the selected arteries or veins. To calculate the blood flow velocity within the capillaries a  $2 \times 2$  square area of pixels was considered. However, for capillaries with vessel diameters less than  $30.4 \mu\text{m}$ , a subset of  $1 \times 1$  square area of pixel size was selected to calculate blood flow velocity. For a  $1 \times 1$  square area of pixel from the SC image, blood flow velocity was not a statistically significant measure since the measurement was based on a single value. Therefore, measurement variance was not reduced by average. These selected subsets of pixels were always inside the vessel diameter.

**Field-of-view (FOV) co-registration image.** The position of imager and animal were fixed for 60 or 66 minutes. Animals were housed overnight at the Animal Resource Center and returned to our laboratory for 24 hours measurements. The field-of-view (FOV) registration was obtained by optical alignment of the SC images at 0 minutes and 24 hours for both experimental and control groups [17–19] to prevent erroneous 24 hours measurements. Specific points in the major arteries and veins of the SC images from 24 hours measurement were co-registered with the SC images from 0 minute. The technique of registering image is illustrated in Figure 6. If the SC images from these two observation points were not optically aligned, the registered image would appear distorted. For the capillaries once the alignment was done, a particular pixel ( $i, j$ ) was selected from the SC image of 60 or 66 minutes which was also valid for 24 hours. For all hamsters, the registered images were found to be optically aligned after the spatial transformation (Fig. 7).

### Statistical Analysis

After PBS or glycerol application, averages were taken for the control ( $n = 6$ ) and experimental ( $n = 7$ ) groups to identify significant changes in blood flow velocity. Variance was calculated by performing standard deviation between all animals at each observation time point for the control and experimental groups. A Bonferroni correction was applied in which a pair-wise comparison was performed for all three separate areas (i.e., artery, vein, and capillary) at each time point.

## RESULTS

### Effect of 100% Anhydrous Glycerol on SC Imaging

Photographs from the sub-dermal and epidermal skin of hamster after flap window implantation are shown in

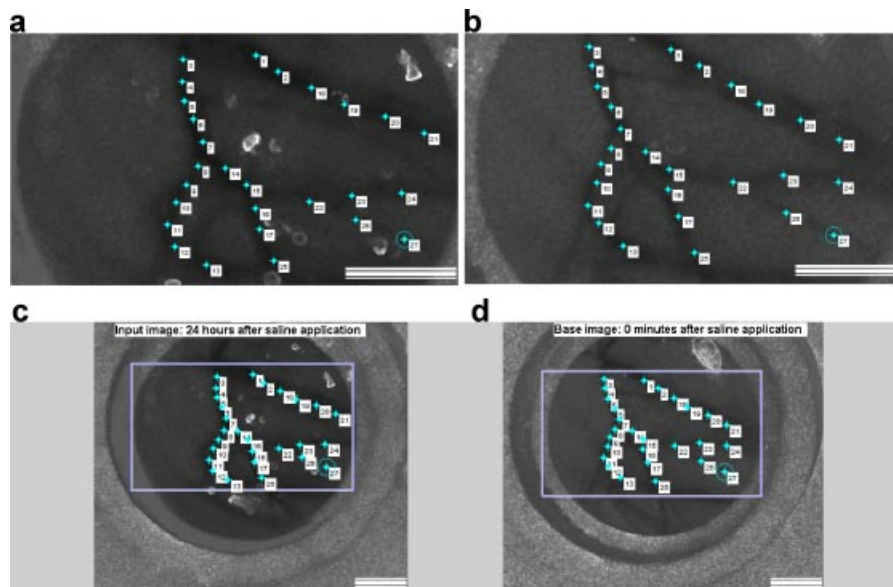


Fig. 6. Registering an SC image at 24 hours as input (c) with base image or 0 minute after saline application (d). **a,b**: Magnified images of input and base SC images, respectively. The control point pairs of the input and base images are highlighted in blue stars and identified with numbers. To get a better resolution minimum of 27 control point pairs was selected in the input and base SC images. The scale bar: 0.25 cm for all four images. [Figure can be viewed in color online via [www.interscience.wiley.com](http://www.interscience.wiley.com).]

Figure 3a,b, respectively. The epidermal side of the skin optically cleared within 3 minutes after treatment with glycerol. The skin remains transparent for at least 66 minutes. The skin was not transparent at 24 hours. Figures 4 and 8–12 illustrate the effect of 100% anhydrous glycerol on blood vessels of hamster's sub-dermal skin. The SC image consisting of  $656 \times 656$  areas of pixels

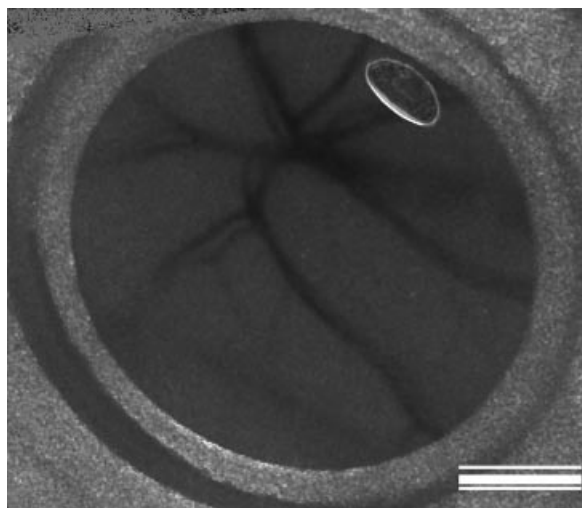


Fig. 7. Registered input and base images after spatial transformation showed an optical alignment between speckle images at 0 minute and 24 hours after saline application. The scale bar: 0.25 cm.

(1 pixel =  $15.2 \mu\text{m}$ ), was computed directly from the raw speckle images using Equation 1 (Figs. 3c–d and 4a–h). The darker areas in the SC image indicate blood flow in the microvasculature.

Figure 4 illustrates time variation in the SC images up to 36 minutes from the sub-dermal side of one of the two hamsters in experimental group E1. Figure 8 is the graphical representation of the SC images of the same hamster shown in Figure 4a–h. Measurement positions are illustrated in Figure 3d. For example, Figure 8a,b, respectively, corresponds to the changes in velocity of an artery (position 2) and two veins (positions 1 and 3), and four capillaries (positions 4, 5, 6, and 13).

One hamster was selected from each experimental group to show typical results on the changes in blood flow velocity (see Figs. 8–10) due to glycerol application. The average changes in blood flow velocity of all seven hamsters of the experimental group with standard deviations are illustrated in Figure 11. Each velocity response is normalized with respect to velocity at 0 minute. Table 1 illustrates the changes in vessel diameter and blood flow velocity of sub-dermal blood vessels due to glycerol application in all seven hamsters of the experimental group. The arteries and veins are both divided in to small and large vessels based on their diameter. The change in diameter is illustrated in Figure 12.

The diameter of both small ( $144\text{--}267 \mu\text{m}$ ) and large ( $321\text{--}336 \mu\text{m}$ ) arteries increased immediately after glycerol application, and then decreased after 12 minutes. The rate of occlusion in small arteries was found to be much higher than for the large arteries. Complete blood flow stoppage

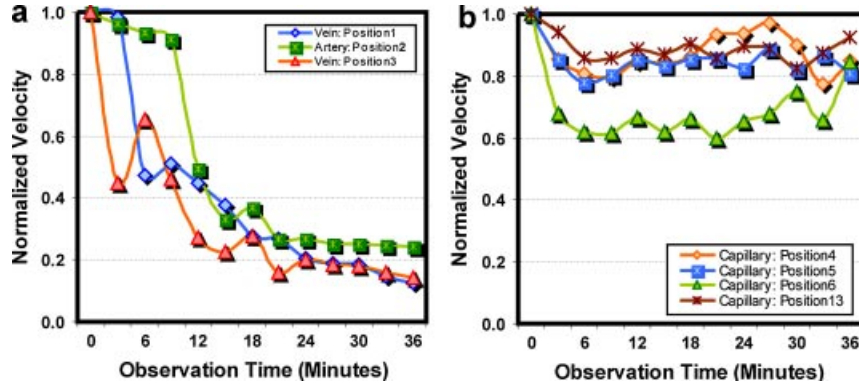


Fig. 8. Normalized velocity of blood perfusion in arteries, veins, and capillaries of one of the two hamster's sub-dermal skin from Group E1 treated with glycerol. Diameter of the artery (position 2) and two veins (positions 1 and 3) are small. The SC images of this hamster are shown in Figure 4. Observation time: 36 minutes. [Figure can be viewed in color online via [www.interscience.wiley.com](http://www.interscience.wiley.com).]

was observed in three out of five small arteries between 57 and 66 minutes after the glycerol application in three hamsters in groups E2 and E3. At 24 hours, small arteries were still slightly dilated and large arteries regained 89% of their baseline diameter. The diameter of both small and large veins varied (see Fig. 12). After the glycerol application, blood flow ceased in all four small veins among four hamsters between 36 and 66 minutes. At 24 hours, the small and large veins regained 74% and 86% of their baseline diameter, respectively.

The blood flow velocity reduced faster in small arteries compared to the large arteries during minutes 9–57. Three out of five small arteries were occluded during 57–66 minutes and the blood flow ceased. No occlusions were identified among large arteries. Although, the average blood flow velocity in the arteries decreased for all seven hamsters after applying hyper osmotic agent (Fig. 11), at 24 hours, the velocity regained 97% of its original flow.

All four small veins with diameter between 249 and 354  $\mu\text{m}$  from four hamsters in the experimental group had a significant reduction in blood flow velocity from 36 to 66 minutes. For example, the dark area corresponding to the position 1 in Figure 4g completely disappeared within 36 minutes in the SC image. Blood flow velocity of veins was further reduced up to 66 minutes compared to 30 minutes measurements (Figs. 9a and 10a). Large veins with diameter 471–600  $\mu\text{m}$  did show some reduction in blood flow velocity without any occlusion. All veins showed a similar reduction in blood velocity as arteries for all seven hamsters after glycerol application (Fig. 11). At 24 hours, blood flow velocity of all veins regained 56% compared to baseline velocity.

Any blood vessels with diameter within 15.2–30.4  $\mu\text{m}$  were considered as capillaries. The blood flow in the capillaries decreased after applying hyper osmotic agent which is illustrated in Figures 8b, 9b, and 10b. An immediate reduction in blood velocity was observed within

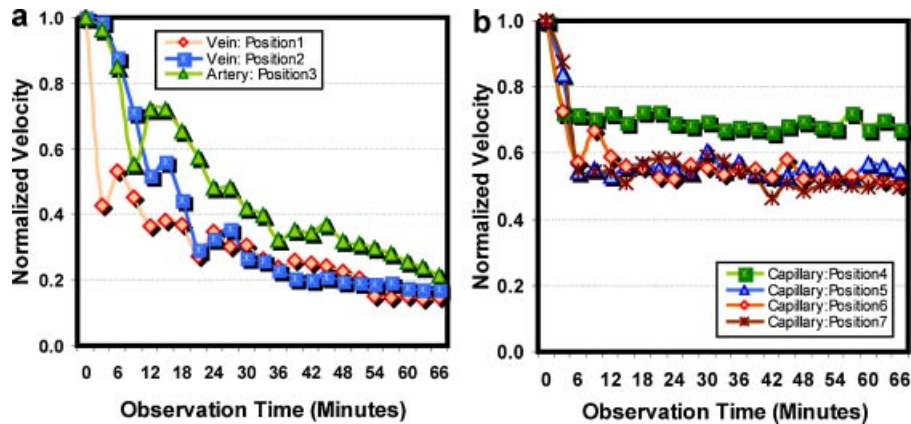


Fig. 9. Normalized velocity of blood perfusion in microvasculatures of one of the two hamster's sub-dermal skin from Group E2 treated with glycerol. The diameter of the artery (position 3) and both veins (positions 1 and 2) are small and large, respectively. Observation time: 66 minutes. [Figure can be viewed in color online via [www.interscience.wiley.com](http://www.interscience.wiley.com).]

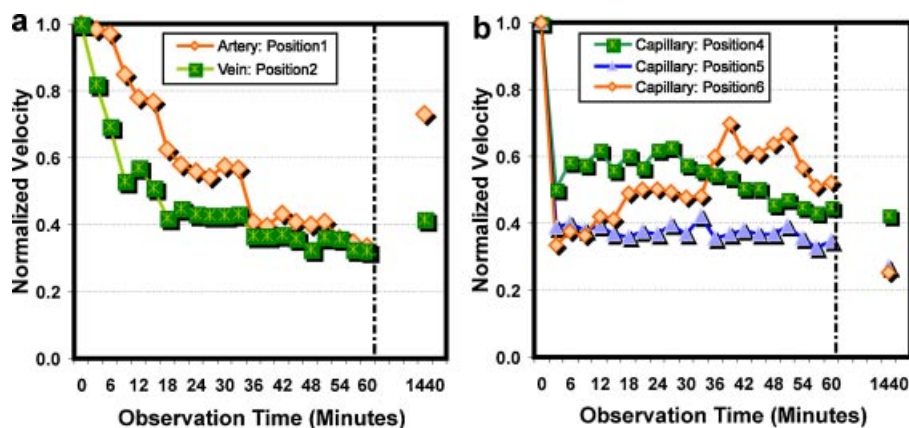


Fig. 10. Normalized velocity of blood perfusion in arteries, veins, and capillaries of one of the three hamster's sub-dermal skin from Group E3 treated with glycerol. The artery (position 1) and vein (position 2) are large in diameter. Observation time: 60 minutes and one measurement at 24 hours. [Figure can be viewed in color online via [www.interscience.wiley.com](http://www.interscience.wiley.com).]

the first 6 minutes after initial glycerol application and stayed unchanged up to 30 minutes. The blood flow velocity in some capillaries continued to decrease at 24 hours compared to 1 hour (Figs. 10b and 11). Table 2 lists the normalized blood flow velocities of arteries, veins, and capillaries which are categorized into experimental groups after skin was treated with glycerol. Each measured blood flow velocity was compared with respect to its baseline velocity at  $t = 0$ . After normalization, the baseline blood flow velocity was specified as a unity (1.0). Standard deviations in Table 2 were with respect to normalized values.

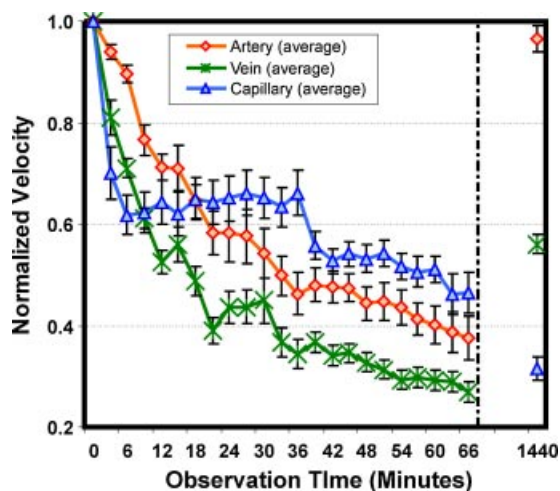


Fig. 11. Average changes in blood flow velocity (normalized) of all arteries, veins, and capillaries due to glycerol application to the sub-dermal skin of 7 hamsters from the experimental group. The standard deviations of the normalized blood flow velocity of arteries, veins, and capillaries are  $\pm 0-0.06$ ,  $\pm 0-0.05$ , and  $\pm 0-0.05$ , respectively. Each response is normalized with respect to its value at  $t = 0$ . [Figure can be viewed in color online via [www.interscience.wiley.com](http://www.interscience.wiley.com).]

### Effect of PBS Solution on SC Imaging

The average change in blood flow velocity of the blood vessels of all six hamsters from control groups C1 and C2 due to application of PBS solution is illustrated in Figure 13. Unlike 100% anhydrous glycerol, the PBS solution slightly increased blood flow velocity of the hamster's sub-dermal microvasculature. In both control groups, the average arterial blood velocity of four out of six hamsters at 3 minutes after applying PBS solution showed an increase (compared to baseline) similar to veins. Unlike veins, the arterial blood velocity exhibited a steady trend that was close to the baseline velocity. A slight decrease in arterial blood velocity was observed between 18 and 33 minutes followed by a gradual increase up to 60 minutes after the initial PBS application. However, the blood flow velocity of arteries, veins, or capillaries did not increase significantly. At 24 hours, all three hamsters from the C2 group demonstrated a slight increase in blood flow velocity among arteries, veins, and capillaries compared to the baseline. However, the increase in the blood flow velocity at any given time was not statistically significant. These statistically non-significant changes in blood flow velocity after applying PBS solution may have been due to some bias caused by surgical trauma or anesthesia.

### DISCUSSION

Although the SC values of the initial native skin (pre-glycerol treatment) blood flow varied among the hamsters, the ratio between the velocity calculated based on correlation time ( $\tau_c$ ) at two different observation time points of the microvasculature was consistent among all seven hamsters of the experimental group over time.

The blood flow velocity of arteries in all seven hamsters decreased at 30 minutes after the initial application of 100% anhydrous glycerol. In this LSCI study, after glycerol application the average diameter of small and large arteries increased up to 9 and 12 minutes, respectively, followed by a decrease. Both of these findings are closely



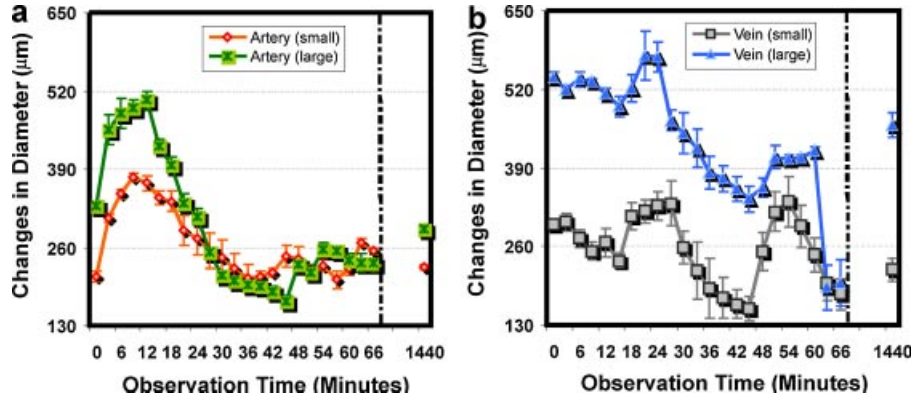


Fig. 12. After applying glycerol the average changes in diameter of the hamster skin blood vessels were measured for arteries and veins. The arteries and vein were classified based on their diameter at baseline. The baseline diameter of arteries was much smaller than veins. The diameters of the small and large arteries ranged between 144–267 and 321–336  $\mu\text{m}$ , respectively. The baseline diameters of the small and large veins were 249–354 and 471–600  $\mu\text{m}$ , respectively. A standard deviation was calculated among small and larger arteries of the hamsters from the experimental group. [Figure can be viewed in color online via [www.interscience.wiley.com](http://www.interscience.wiley.com).]

correlated with the findings of a previous DOCT studies by Vargas et al. and Barton et al. [3,20,21]. In the DOCT study, the arterial diameter increased up to 10 minutes.

Our results illustrate that the blood velocity of veins was reduced faster and more significantly than arteries. The velocity decreased in small veins to such an extent that the dark area of a SC image due to blood flow, disappeared completely within 36 minutes after applying 100% anhydrous glycerol. We also observed small arteries occluded along with cessation of blood flow velocity at 57 minutes from initial glycerol application. This occlusion was due to small vein's thin vessel wall compared to artery's lumen diameter. Thus, the chemical diffusion dynamics occurred faster in veins than arteries. This finding verified results from the DOCT study, where Doppler images showed glycerol enhanced trans-dermal visualization of blood vessels along with cessation of blood flow in veins and sometimes in arteries [3].

The decrease in blood flow induced by glycerol could be due to an inflammatory response by the tissue in response to osmotic equilibrium deviations. In an acute inflammatory response, blood vessels are subjected to increased permeability and plasma exits into the extra-vascular network [22,23]. Moreover, in native blood vessels, the majority of blood cells are concentrated in the center of the stream, with an increased concentration of plasma near the lumen wall [22]. This characteristic is important in keeping the viscosity near the lumen wall at a minimum so that peripheral resistance is lower than it would be if the cells were uniformly distributed. If plasma is lost to the extra-vascular network due to osmotic pressure incurred by 100% anhydrous glycerol, this property is lost and the flow in the blood vessels is reduced because there is greater drag on the lumen walls [22].

The diameter of small arteries and veins decreased along with reduction in blood flow velocity. Thus, the

change in diameter and reduction in blood velocity may have a direct correlation. For example, in Figure 3d, Position 1 (diameter 144  $\mu\text{m}$ ) and position 3 (diameter 567  $\mu\text{m}$ ) are both veins, only position 1 has a significant reduction in blood velocity (see the gradual changes of dark area in Fig. 4a–h). The dark area representing position 1 disappears completely in Figure 4h. This effect may be caused by an increased clearing of the tissue overlying the vessels and could also occur with vasoconstriction.

Some of the small arteries and veins with 2.3–2.4 $\times$  smaller diameter compared to large microvasculature showed a major reduction in blood flow velocity with complete cession. At 30 minutes after glycerol application, the average velocity of the small arteries decreased 60.0% compared to the large arteries whose velocity reduced only 27.0%. Three out of five small arteries completely occluded between 57 and 66 minutes. At 30 minutes, the average blood flow velocity of small veins reduced 68% compared to 45% in large veins. Blood flow in majority of small veins (4 out of 5) ceased at 36 minutes which was much earlier than small arteries. At 24 hours, the arteries and veins respectively regained 97% and 56% of their original blood velocity. A *t*-test with 95% confidence interval showed that the regained velocity of arteries compared to baseline is not statistically significant. However, the blood flow velocity of veins at 24 hours is significant. These results established that arteries can completely reverse the effect of a hyperosmotic agent without any sub-dermal skin hydration with 0.9% saline.

The reason for this recovery of blood flow velocity in arteries and veins without saline may due to one side of the epidermal skin being intact during the experiment. The *in vivo* skin of hamsters can rapidly hydrate this microvasculature. Wang and Tuchin reported optical clearing by topical sub-dermal application of glycerol was reversible

**TABLE 1. Average Changes in Diameter of Blood Vessels and Normalized Blood Flow Velocity Due to Hyper-Osmotic Agent With Standard Deviation**

Time (minutes)	Arteries ( $n = 14$ )				Veins ( $n = 11$ )			
	Small: 144–267 $\mu\text{m}$ ( $n = 8$ )		Large: 321–336 $\mu\text{m}$ ( $n = 6$ )		Small: 249–354 $\mu\text{m}$ ( $n = 5$ )		Large: 471–600 $\mu\text{m}$ ( $n = 6$ )	
	Diameter	Normalized velocity	Diameter	Normalized velocity	Diameter	Normalized velocity	Diameter	Normalized velocity
0	211 $\pm$ 8	1.00 $\pm$ 0.00	328 $\pm$ 2	1.00 $\pm$ 0.00	298 $\pm$ 6	1.00 $\pm$ 0.00	540 $\pm$ 9	1.00 $\pm$ 0.00
3	308 $\pm$ 6	0.92 $\pm$ 0.02	455 $\pm$ 25	0.96 $\pm$ 0.02	301 $\pm$ 15	0.79 $\pm$ 0.03	519 $\pm$ 8	0.82 $\pm$ 0.04
6	349 $\pm$ 8	0.90 $\pm$ 0.01	483 $\pm$ 25	0.91 $\pm$ 0.03	273 $\pm$ 16	0.67 $\pm$ 0.02	537 $\pm$ 12	0.75 $\pm$ 0.02
9	376 $\pm$ 6	0.74 $\pm$ 0.04	493 $\pm$ 12	0.84 $\pm$ 0.01	252 $\pm$ 14	0.58 $\pm$ 0.03	533 $\pm$ 5	0.63 $\pm$ 0.02
12	367 $\pm$ 13	0.65 $\pm$ 0.03	504 $\pm$ 15	0.82 $\pm$ 0.01	267 $\pm$ 23	0.49 $\pm$ 0.03	512 $\pm$ 10	0.55 $\pm$ 0.02
15	343 $\pm$ 11	0.64 $\pm$ 0.06	429 $\pm$ 9	0.87 $\pm$ 0.02	236 $\pm$ 12	0.45 $\pm$ 0.03	492 $\pm$ 17	0.65 $\pm$ 0.04
18	336 $\pm$ 16	0.62 $\pm$ 0.05	398 $\pm$ 12	0.75 $\pm$ 0.02	311 $\pm$ 22	0.40 $\pm$ 0.03	522 $\pm$ 23	0.56 $\pm$ 0.03
21	288 $\pm$ 25	0.49 $\pm$ 0.04	334 $\pm$ 15	0.74 $\pm$ 0.03	319 $\pm$ 19	0.36 $\pm$ 0.02	576 $\pm$ 40	0.41 $\pm$ 0.03
24	274 $\pm$ 27	0.45 $\pm$ 0.03	311 $\pm$ 14	0.81 $\pm$ 0.06	328 $\pm$ 24	0.36 $\pm$ 0.03	574 $\pm$ 24	0.50 $\pm$ 0.03
27	255 $\pm$ 29	0.45 $\pm$ 0.04	252 $\pm$ 4	0.79 $\pm$ 0.05	331 $\pm$ 37	0.36 $\pm$ 0.04	468 $\pm$ 17	0.50 $\pm$ 0.03
30	244 $\pm$ 27	0.40 $\pm$ 0.03	214 $\pm$ 4	0.73 $\pm$ 0.04	259 $\pm$ 27	0.32 $\pm$ 0.03	448 $\pm$ 34	0.55 $\pm$ 0.06
33	225 $\pm$ 24	0.39 $\pm$ 0.03	206 $\pm$ 7	0.68 $\pm$ 0.02	221 $\pm$ 47	0.34 $\pm$ 0.03	423 $\pm$ 31	0.48 $\pm$ 0.03
36	210 $\pm$ 23	0.38 $\pm$ 0.04	199 $\pm$ 8	0.65 $\pm$ 0.03	190 $\pm$ 49 <sup>b</sup>	0.32 $\pm$ 0.03	382 $\pm$ 27	0.45 $\pm$ 0.03
39	212 $\pm$ 8	0.38 $\pm$ 0.01	197 $\pm$ 8	0.58 $\pm$ 0.03	175 $\pm$ 34 <sup>b</sup>	0.32 $\pm$ 0.03	372 $\pm$ 21	0.36 $\pm$ 0.02
42	218 $\pm$ 7	0.37 $\pm$ 0.01	187 $\pm$ 9	0.58 $\pm$ 0.03	164 $\pm$ 24 <sup>b</sup>	0.32 $\pm$ 0.03	356 $\pm$ 20	0.32 $\pm$ 0.01
45	246 $\pm$ 18	0.40 $\pm$ 0.01	170 $\pm$ 11	0.55 $\pm$ 0.03	157 $\pm$ 20 <sup>b</sup>	0.32 $\pm$ 0.03	338 $\pm$ 22	0.33 $\pm$ 0.01
48	241 $\pm$ 19	0.35 $\pm$ 0.01	232 $\pm$ 8	0.54 $\pm$ 0.03	252 $\pm$ 32 <sup>b</sup>	0.31 $\pm$ 0.03	357 $\pm$ 15	0.31 $\pm$ 0.01
51	221 $\pm$ 10	0.31 $\pm$ 0.00	219 $\pm$ 12	0.56 $\pm$ 0.04	318 $\pm$ 32 <sup>b</sup>	0.31 $\pm$ 0.03	407 $\pm$ 19	0.30 $\pm$ 0.01
54	230 $\pm$ 15	0.32 $\pm$ 0.01	258 $\pm$ 10	0.55 $\pm$ 0.03	334 $\pm$ 41 <sup>b</sup>	0.30 $\pm$ 0.03	404 $\pm$ 8	0.30 $\pm$ 0.01
57	206 $\pm$ 14 <sup>a</sup>	0.31 $\pm$ 0.01	254 $\pm$ 5	0.52 $\pm$ 0.03	294 $\pm$ 35 <sup>b</sup>	0.29 $\pm$ 0.02	406 $\pm$ 5	0.30 $\pm$ 0.01
60	225 $\pm$ 12 <sup>a</sup>	0.25 $\pm$ 0.01	239 $\pm$ 11	0.53 $\pm$ 0.03	246 $\pm$ 28 <sup>b</sup>	0.29 $\pm$ 0.03	418 $\pm$ 7	0.29 $\pm$ 0.01
63	267 $\pm$ 7 <sup>a</sup>	0.22 $\pm$ 0.01	233 $\pm$ 15	0.52 $\pm$ 0.04	200 $\pm$ 29 <sup>b</sup>	0.25 $\pm$ 0.03	193 $\pm$ 37	0.29 $\pm$ 0.02
66	253 $\pm$ 20 <sup>a</sup>	0.20 $\pm$ 0.00	233 $\pm$ 11	0.51 $\pm$ 0.04	181 $\pm$ 26 <sup>b</sup>	0.21 $\pm$ 0.03	200 $\pm$ 38	0.27 $\pm$ 0.02
1440	228 $\pm$ 4	0.82 $\pm$ 0.00	291 $\pm$ 6	0.99 $\pm$ 0.03	221 $\pm$ 19	0.51 $\pm$ 0.02	462 $\pm$ 20	0.61 $\pm$ 0.02

$n$  is the total number of blood vessels, which were chosen in each experimental group to calculate blood flow velocity.  $n$  is not same for each observation time for arteries ( $n_a$ ) and veins ( $n_v$ ): (i) between 0 and 36 minutes  $n_a = 14$  (S:8, L:6) and  $n_v = 11$  (S:5, L:6); (ii) between 36 and 60 minutes  $n_a = 11$  (S:5, L:6) and  $n_v = 8$  (S:4, L:4); (iii) at 24 hours  $n_a = 7$  (S:1, L:6) and  $n_v = 4$  (S:2, L:2), where S and L represent the number of small and large blood vessels, respectively. Table 2 listed the total  $n$  for each experimental group.

<sup>a</sup>Three hamsters in the experimental group had complete blood vessel occlusion in the small arteries.

<sup>b</sup>Four hamsters in the experimental group had complete blood vessel occlusion in the small veins.

and under certain conditions may not damage skin once the tissue was hydrated [24]. At 24 hours, we observed some hamster's sub-dermal tissue dehydrated even after the sub-dermal side of the skin was covered with a round piece of glass. To avoid tissue dehydration it was necessary to apply saline to the tissue.

These observed morphological effects of glycerol will likely aid to permanent laser destruction of blood vessels of cutaneous vascular lesions. Specifically, decreased peripheral blood flow velocity induced by glycerol will facilitate permanent destruction of blood vessels using laser irradiation, particularly in those situations where high velocity of blood flow compromises the effectiveness of laser irradiation. Previous studies have shown that complete flow cessation in blood vessels before irradiation significantly reduces the fluence rate ( $\text{W}/\text{cm}^2$ ), which is required to destroy the vessel permanently [25].

This study further showed that the blood flow velocity in capillaries of treated sub-dermal skin reduced faster than in either an artery or a vein. This effect was due to capillary's thinnest vessel wall compared to arteries and veins. In a capillary, the effect was more significant since only one to two red blood cells can pass through the vessel at a given time. Hundred percent anhydrous glycerol increased viscosity and had a long-term effect with less recovery [3,20]. Within 3 minutes after initial glycerol application, the blood flow velocity in all capillaries decreased by 30%. Unlike arteries and veins, capillaries velocity continuously decreased up to 24 hours.

One possible hypothesis for this phenomenon is that the local blood velocity in capillaries is mediated by nitric oxide (NO), whereas flow in arteries and veins is at least partially regulated by the autonomic nervous system (ANS). Thus, the ANS can override the effect of topical application of

**TABLE 2. Relative Blood Flow Velocity of the Microvasculatures in the Experimental Group Hamster's Sub-Dermal Skin Due to 100% Anhydrous Glycerol Application**

Observation time	3-minute	½ hour	1 hour	24 hours
Arteries (average ± standard deviation)				
E1 ( <i>n</i> = 3)	0.962 ± 0.016	0.254 ± 0.023	—	—
E2 ( <i>n</i> = 4)	0.961 ± 0.001	0.416 ± 0.022	0.254 ± 0.012	—
E3 ( <i>n</i> = 7)	0.916 ± 0.018	0.739 ± 0.037	0.486 ± 0.039	0.966 ± 0.034 <sup>a</sup>
All groups	0.938 ± 0.016	0.543 ± 0.046	0.402 ± 0.038	—
Veins (average ± standard deviation)				
E1 ( <i>n</i> = 3)	0.714 ± 0.047	0.183 ± 0.002	—	—
E2 ( <i>n</i> = 4)	0.706 ± 0.049	0.286 ± 0.003	0.161 ± 0.003	—
E3 ( <i>n</i> = 4)	0.984 ± 0.036	0.813 ± 0.049	0.424 ± 0.013	0.561 ± 0.019
All groups	0.809 ± 0.034	0.449 ± 0.045	0.292 ± 0.019	—
Capillaries (average ± standard deviation)				
E1 ( <i>n</i> = 8)	0.832 ± 0.027	0.825 ± 0.015	—	—
E2 ( <i>n</i> = 7)	0.790 ± 0.019	0.612 ± 0.015	0.564 ± 0.019	—
E3 ( <i>n</i> = 10)	0.618 ± 0.021	0.550 ± 0.003	0.473 ± 0.022	0.316 ± 0.023
All groups	0.701 ± 0.052	0.651 ± 0.041	0.510 ± 0.025	—

*n* is the total number of blood vessels that were chosen in each experimental group to calculate blood flow velocity.

<sup>a</sup>Not a significant change ( $P < 0.05$ ) based on ANOVA *t*-test.

glycerol on blood velocity of arteries and veins. Another possible hypothesis is that the much smaller cross-sectional area of capillaries is very quickly and easily affected by the hyper-osmotic agent. Burek et al. [26] states that the reduction of blood flow velocity in the microvasculature such as arteries is due to an inhibition of NO biosynthesis. The study further showed that NO is important for functional hyperemia (vasodilatation) of the cat optic nerve head (ONH) microcirculation during increased neural activity with flickering light stimuli to the eye [25]. Wang

et al. [27] agrees that NO clearly plays a role in regulating blood flow to the dog ophthalmic arteries. Thus, the changes in blood flow velocity and diameter of the microvasculature may have direct correlation with the inhibition of NO biosynthesis after the hamster's sub-dermal skin is treated with 100% anhydrous glycerol. In the LSCI study, blood vessels dilated in the beginning of the glycerol treatment, which could be due to the availability of NO to the microvasculature. However, while time progressed the NO biosynthesis is inhibited and the microvasculature is forced to constrict along with reduction in blood flow velocity. In a previous study, Bertuglia et al. [28] measurements on dynamic arteriolar diameter changes from skeletal muscle in conscious hamsters demonstrate that NO is not required for vasomotion in the skeletal muscle of conscious animals. Bertuglia's study further validates the findings of this LSCI study that the NO definitely plays a role in vasomotion or regulating the diameter of the microvasculatures of the hamster's sub-dermal skin when the hamsters are under deep anesthetic and completely unconscious. Further investigation is needed to confirm either of these hypotheses.

A statistical analysis was performed for all blood flow velocity data collected from the seven hamsters of the experimental group. The Bonferroni correction was applied to the interaction decomposition in which a pair wise comparison is performed for all three separate areas (i.e., artery, vein, and capillary) at each time point [29–31]. A statistical significance ( $P < 0.05$ ) was observed in the difference in blood velocity between an artery and a capillary, and a vein and a capillary at 12 minutes after the initial application of glycerol. However, the changes in blood flow velocity of arteries and veins of all seven hamsters showed no significance during 0–66 minutes except for at 24 hours. At 24 hours, arteries normalized

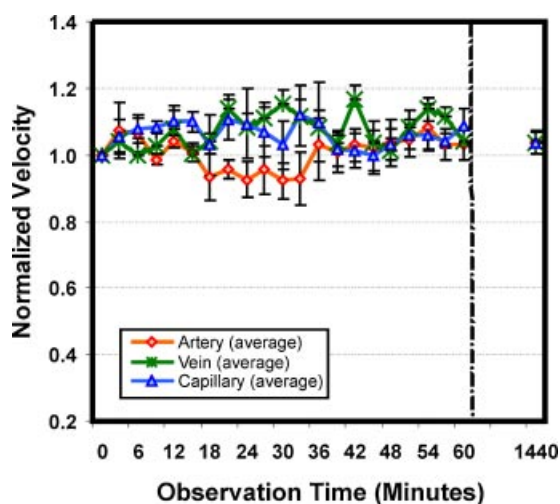


Fig. 13. Normalized average blood velocity of all six hamster's sub-dermal skin blood vessels after saline application. Variance of blood flow velocity was calculated by standard deviation of all hamsters of individual groups for each observation time. Observation time: 60 minutes and one measurement at 24 hours.

average blood flow velocity was not significant with respect to baseline unlike veins.

The accuracy of these relative changes in blood flow velocity and blood vessel diameter may have impacted by surgical trauma and effects of anesthesia. The FOV co-register and LSCI sampling error may also introduce uncertainty. In all likelihood, the changes that are observed in this study are probably due to a combination of multiple physiological processes induced by glycerol application.

## CONCLUSION

Glycerol was found to decrease the blood flow velocity of veins and to some degree of arteries within 1 hour after the initial application of glycerol. Although, at 24 hours recovery of blood flow velocity was observed without hydrating the glycerol treated skin with PBS or 0.9% saline, unlike arteries veins did not regained normal velocity. Also, capillaries did not return to normal flow compared to pre-glycerol treatment. A further study on capillary treated with glycerol can be done using a 2-photon microscope that could validate and quantify the absolute blood flow velocity at 24 hours. The glycerol application also caused an immediate increase in blood vessel diameter followed by a reduction in diameter within 1 hour. At 24 hours, arteries and veins regained their original vessel diameter. Further studies are required to evaluate the two hypothesis presented in this study to identify the underline causes for blood flow velocity to reduce along with decrease in vessel diameter after application of 100% anhydrous glycerol.

## ACKNOWLEDGMENTS

This research has been supported by the National Science Foundation (UTA06-688) and Caster Foundation. Raiyan Zaman was a recipient of the Air Force Academy Travel Grant to attend ASLMS conference, 2008. Special thanks to Dr. Gracie Vargas for teaching Raiyan the technique for implanting the window model on hamster.

## REFERENCES

- Vargas G, Chan EK, Barton JK, Rylander HG III, Welch AJ. Use of an agent to reduce scattering in skin. *Lasers Surg Med* 1999;24:133–141.
- Ghosn MG, Tuchin VV, Larin KV. Depth-resolved monitoring of glucose diffusion in tissues by using optical coherence tomography. *Opt Lett* 2006;31(15):2314–2316.
- Vargas G, Readinger A, Dozier SS, Welch AJ. Morphological changes in blood vessels produced by hyper osmotic agents and measured by optical coherence tomography. *Photochem Photobiol* 2003;77(5):541–549.
- Bakutkin VV, Maksimova IL, Semyonova TN, Tuchin VV, Kon IL. Controlling of optical properties of sclera. *Proc SPIE* 1995;2393:137–141.
- Tuchin VV, Maksimova IL, Zimnyahkov DA, Kon IL, Mavlutov AK, Mishin AA. Light propagation in tissues with controlled optical properties. *Proc SPIE* 1996;2925:118–142.
- Tuchin VV, Maksimova IL, Zimnyakov DA, Kon IL, Mavlutov AK, Mishin AA. Light propagation in tissues with controlled optical properties. *J Biomed Opt* 1997;2:401–417.
- Vargas G, Chan KF, Thomsen SL, Welch AJ. Use of osmotically active agents to alter optical properties of tissue: Effects on the detected fluorescence signal measured through skin. *Lasers Surg Med* 2001;29:213–220.
- Choi B, Ramirez-San-Juan JC, Lotfi J, Nelson JS. Linear response range characterization and in vivo application of laser speckle imaging of blood flow dynamics. *J Biomed Opt* 2006;11(4):041129.
- Zhu D, Zhang J, Cui H, Mao Z, Li P, Luo Q. Short-term and long-term effects of optical clearing agents on blood vessels in chick chorioallantoic membrane. *J Biomed Opt* 2008;13(2):021106.
- Briers JD, Webster S. Laser speckle contrast analysis (LASCA): A non-scanning, full-field technique for monitoring capillary blood flow. *J Biomed Opt* 1996;1:174–179.
- Dunn AK, Bolay H, Moskowitz MA, Boas DA. Dynamic imaging of cerebral blood flow using laser speckle. *J Cereb Blood Flow Metab* 2001;21:195–201.
- Fercher A, Briers J. Flow visualization by means of single exposure speckle photography. *Opt Commun* 1981;37:326–329.
- Yuan S, Devor A, Boas DA, Dunn AK. Determination of optical exposure time for imaging of blood flow changes with laser speckle contrast imaging. *Appl Opt* 2005;44(10):1823–1830.
- Papenfuss HD, Gross JF, Intaglietta M, Treese FA. A transparent access chamber for the rat dorsal skin flap. *Microvasc Res* 1979;18:311–318.
- Dunn AK, Bolay H, Moskowitz MA, Boas DA. Dynamic imaging of cerebral blood flow using laser speckle. *J Cereb Blood Flow Metab* 2001;21:195–201.
- Boyle R, Thomas R. *Computer vision: A first course*. Blackwell Scientific Publications, Oxford, England, 1988. Chapter 5.
- Shams R, Barnes N, Harley R. Image registration in Hough space using gradient of images. *IEEE Xplore Digital Image Comput Tech Appl* 2007;226–232.
- Chunhavitayatera S, Chitsobhuk O, Tongprasert K. Image registration using Hough transform and phase correlation. *Int Conf Adv Commun Technol (ICACT)* 2006;(2):973–977.
- Cole-Rhodes A, Johnson K, LeMoigne J, Zavorin I. Multi-resolution registration of remote sensing imagery by optimization of mutual information using a stochastic gradient. *IEEE Trans Image Processing* 2003;12(12):1495–1511.
- Vargas G. Reduction of light scattering in biological tissue: Implications for optical diagnostics and therapeutics. Doctoral Dissertation 2001; The University of Texas at Austin.
- Barton JK. Predicting dosimetry for laser coagulation of in vivo cutaneous blood vessels. Doctoral Dissertation 1998; The University of Texas at Austin.
- Wahl LM, Wahl SM. Inflammation. In: Cohen IK, Diegelmann RF, Lindblad WJ, editors. *Wound healing, biochemical and clinical aspects*. Philadelphia: W.B. Saunders Co.; 1992. pp. 40–53. [Chapter 3].
- Walter JB, Israel MS. The inflammatory reaction. In: Walter JB, editor. *General pathology*. 4th edition. London: Churchill Livingstone; 1974. pp. 69–83. [Chapter 6].
- Wang RK, Tuchin VV. Tissue clearing as a tool to enhance imaging capability for optical coherence tomography. *Proc SPIE* 2002;4619:22–25.
- Boergen KP, Birngruber R, Gabel VP, Hillenkamp F. Experimental studies on controlled closure of small vessels by laser irradiation. *Proc Lasers Surg Med Biol (Munich)* 1977;5:15.
- Burek DG, Riva CE. Vasomotion and spontaneous low-frequency oscillations in blood flow and nitric oxide in cat optic nerve head. *Microvasc Res* 1998;55:103–112.
- Wang Y, Okamura T, Toda N. Mechanism of acetyl-choline-induced relaxation in dog external and internal ophthalmic arteries. *Exp Eye Res* 1993;57:275–282.
- Bertuglia S, Colantuoni A, Dunn R, Jr. Effect of L-NMMA and indomethacin on arteriolar vasomotion in skeletal muscle microcirculation of conscious and anesthetized hamsters. *Microcirc Res* 1994;48:68–84.
- Abdi H. In: The Bonferroni and Sidak corrections for multiple comparisons. Salkind NJ, editor. *Encyclopedia of measurement and statistics*. Thousand Oaks, CA: Sage; 2007.
- Miller RG, Jr. *Simultaneous statistical inference*. New York: Springer Verlag; 1991.
- Shaffer JP. Multiple hypothesis testing. *Ann Rev Psych* 1995;46:561–584.